

Mechanical control of heat conductivity in molecular chainsA. V. Savin^{1,*} and O. V. Gendelman^{2,†}¹*Semenov Institute of Chemical Physics, Russian Academy of Sciences, Moscow 119991, Russia*²*Faculty of Mechanical Engineering, Technion—Israel Institute of Technology, Haifa 32000, Israel*

(Received 6 October 2013; published 22 January 2014)

We discuss a possibility to control heat conductivity in molecular chains by means of external mechanical loads. To illustrate such possibilities we consider first well-studied one-dimensional chain with degenerate double-well potential of the nearest-neighbor interaction. We consider varying lengths of the chain with fixed number of particles. Number of possible energetically degenerate ground states strongly depends on the overall length of the chain, or, in other terms, on average length of the link between neighboring particles. These degenerate states correspond to mechanical equilibria; therefore, one can say that formation of such structures mimics a process of plastic deformation. We demonstrate that such modification of the chain length can lead to quite profound (almost fivefold) reduction of the heat conduction coefficient. Even more profound effect is revealed for a model with a single-well nonconvex potential. It is demonstrated that in a certain range of constant external forcing, this model becomes effectively double-well and has a multitude of possible states of equilibrium for fixed value of the external load. Due to this degeneracy, the heat-conduction coefficient can be reduced by two orders of magnitude. We suggest a mechanical model of a chain with periodic double-well potential, which allows control of the heat transport. The models considered may be useful for description of heat transfer in biological macromolecules and for control of the heat transport in microsystems. The possibility of the heat transport control in more realistic three-dimensional systems is illustrated by simulation of a three-dimensional model of polymer α -helix. In this model, the mechanical stretching also brings about the structural inhomogeneity and, in turn, to essential reduction of the heat conductivity.

DOI: [10.1103/PhysRevE.89.012134](https://doi.org/10.1103/PhysRevE.89.012134)

PACS number(s): 44.10.+i, 05.45.-a, 05.60.-k, 05.70.Ln

I. INTRODUCTION

Heat conduction in low-dimensional systems has attracted a lot of attention and has been a subject of intensive studies [1,2]. The main objective here is to substantiate from the first principles the Fourier law—proportionality of the heat flux to the temperature gradient $J = -\kappa \nabla T$, where κ is the heat conduction coefficient. To date, there exists quite an extensive body of works devoted to the numerical modeling of the heat transfer in the one-dimensional chains. Anomalous characteristics of this process are well known since the celebrated work of Fermi, Pasta, and Ulam [3]. In integrable systems (harmonic chain, Toda lattice, the chain of rigid disks) the heat flux J does not depend at all on the chain length L , therefore, the thermal conductivity formally diverges. The underlying reason for that is that the energy is transferred by noninteracting quasiparticles, and therefore one cannot expect any diffusion effects. Nonintegrability of the system is a necessary but not sufficient condition to obtain the convergent heat-conduction coefficient. Well-known examples are the Fermi-Pasta-Ulam (FPU) chain [4–6], disordered harmonic chain [7–9], diatomic 1D gas of colliding particles [10–12], and the diatomic Toda lattice [13]. In these, nonintegrable systems also have divergent heat conduction coefficient; the latter diverges as a power function of length: $\kappa \sim L^\alpha$, for $L \rightarrow \infty$. The exponent is nonuniversal and lies in the interval $0 < \alpha < 1$.

On the other side, the 1D lattice with onsite potential can have finite heat conductivity. The simulations had demon-

strated the convergence of the heat-conduction coefficient for Frenkel-Kontorova chain [14,15], the chain with hyperbolic sine onsite potential [16], the chain with ϕ^4 onsite potential [17,18], and for the chain of hard disks of nonzero size with substrate potential [19]. An essential feature of all these models is an existence of external potential modeling the interaction with the surrounding system. These systems are not translationally invariant, and, consequently, the total momentum is not conserved. In Ref. [14] it has been suggested that the presence of an external potential plays a key role to ensure the convergence of the heat conductivity. This hypothesis has been disproved in Refs. [20,21], where it was shown that the isolated chain of rotators (a chain with a periodic potential of the nearest-neighbor interaction) has the convergent thermal conductivity.

In recent papers [22,23], the thermal conductivity of an isolated chain with asymmetric nearest-neighbor potential was studied. The authors claimed that with a certain degree of interaction asymmetry, the thermal conductivity measured in nonequilibrium conditions converges in the thermodynamical limit. The authors of Refs. [22,23] attribute the convergence of the thermal conductivity to the uneven thermal expansion of the asymmetric chain. More detailed investigation undertaken in Refs. [24–26] pointed out that this numeric conclusion is wrong in thermodynamic limit and is caused by finite-size effects. Indeed, the heat conductivity in the α - β -Fermi-Pasta-Ulam chain diverges [24,25]. It seems that the asymmetry of the nearest-neighbor potential is insufficient to provide the convergence; however, possibility of the chain dissociation might be sufficient [26].

In the systems mentioned above, the strong nonhomogeneities, which critically effect the heat transfer, are conjectured to be caused by the thermal fluctuations. In the current

*asavin@center.chph.ras.ru

†ovgend@tx.technion.ac.il

work, we would like to explore a somewhat different idea—to design the interaction potential and external conditions in a way that the inhomogeneities will appear in a controllable manner and with desired density. Thus, it might be possible to control the heat-conduction coefficient in wide range by simple variation of the external conditions—for instance, by stretching the chain.

Modification of the heat conduction by mass loading of certain nanostructures has been revealed in a number of recent experiments [27,28]. We would like to pursue here a more systematic study with a simple model and to figure out the basic mechanism responsible for these phenomena. In order to accomplish this goal, we study a chain with a double-well (DW) potential of the nearest-neighbor interactions. We also study certain modification of the DW model, which has only one minimum but can acquire the double-well structure under action of external force. These systems are studied both under nonequilibrium conditions using Langevin thermostats and within the framework of equilibrium molecular dynamics using Green-Kubo formula [29].

The main results presented in this paper were obtained for one-dimensional models. To assess to some extent the effects caused by higher dimensionality, we also consider the stretching-induced modification of heat transfer in a three-dimensional model of polymer α -helix.

The thermal conductivity of the chain with double-well potential was considered in Ref. [20], with the help of nonequilibrium molecular-dynamics simulation with Nose-Hoover thermostats. It was shown that the use of Nose-Hoover thermostat for the nonequilibrium problems can be misleading [30,31]. More accurate modeling of the heat transfer using Langevin thermostat was presented in Ref. [32]. It seems that neither of these previous works considered the relationship between the variations of the chain length and the thermal conductivity. An important feature of the chain with the DW potential is the existence of a large number of possible ground states of the chain. So, the chain with N particles and periodic boundary conditions has 2^{N-1} possible ground states with the same energy; the only possible difference between these states is the overall equilibrium length of the chain. We show that the thermal conductivity of the chain depends essentially on its ground state, governed by the length. At least, it happens when the temperature is not much higher than the potential barrier—in the regime of high temperatures the details of potential relief will become less important. In each particular simulation, the overall length of the chain is fixed, and all ground states corresponding to this particular value of the length are considered to be equivalent. So, we are going to show that the variation of the chain length brings about significant change of its thermal conductivity. We also show that the same (and even much stronger) effect can be achieved for special design of a single-well nearest-neighbor potential; in this case, the multiplicity of the ground states is achieved by application of a uniform external stretching. Besides, we demonstrate that also the phenomena related to a nonequilibrium heat conduction, like relaxation modes of thermal perturbations, are strongly affected by the number of competing ground states

It should be mentioned that the heat conduction coefficient of some models considered in this paper is believed to

be divergent in the thermodynamic limit. This point is not significant here, since we discuss the effect of length, stretching, and number of the ground states in a chain with fixed number of particles. Therefore, the heat conduction coefficient is well-defined in all considered cases.

II. DESCRIPTION OF THE MODEL

Let us consider a chain with N particles. In a dimensionless form the Hamiltonian of the chain can be written as

$$H = \sum_{n=1}^N \frac{1}{2} \dot{u}_n^2 + \sum_{n=1}^{N-1} V(u_{n+1} - u_n), \quad (1)$$

where N is the total number of particles in the chain, u_n is a coordinate of the n th particle, dot denotes differentiation with respect to dimensionless time t , $V(\rho_n)$ is the nearest-neighbor interaction potential, and $\rho_n = u_{n+1} - u_n$ is the length of the n th link between the neighboring particles. The coordinate of the particle u_n cannot only describe the position of the particles with respect to the chain axis; it may also correspond to the rotation angle of the n th monomer around the rotation axis. In this sort of model, ρ_n will denote the relative angle between the $(n+1)$ th and the n th monomer.

We choose the double-well (DW) potential of the interparticle interaction in the following form:

$$V(\rho) = \epsilon(\rho - 1)^2(\rho - 2)^2, \quad (2)$$

where we choose $\epsilon = 1/2$; it leads to $V''(1) = V''(2) = 1$. The shape of the potential is presented in Fig. 1. The height of the barrier between the minima of the potential $E_0 = V(1.5) = 1/2^5 = 0.0313$. Such a model can, for instance, describe a polymer macromolecule with two energetically degenerate gauche states.

To simulate the heat transfer in the chain, we use the stochastic Langevin thermostat. The chain has in general $N_+ + N + N_-$ particles. We connect N_+ particles from one side of the chain to a “hot” Langevin thermostat with temperature T_+ , and N_- particles from the other side—to the Langevin

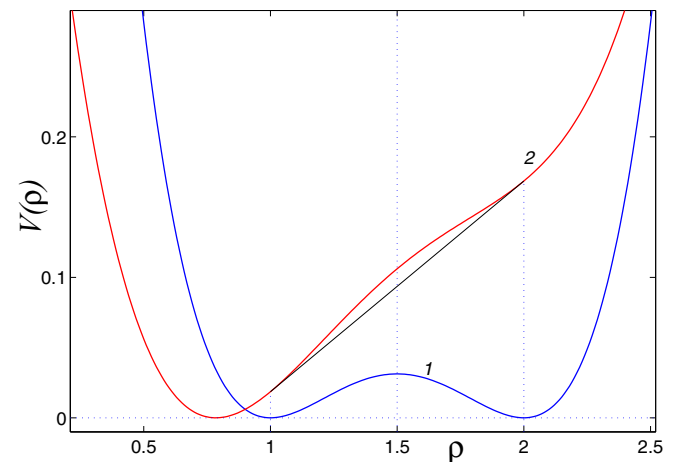


FIG. 1. (Color online) Sketch of double-well potential Eq. (2) (curve 1) and single-well potential Eq. (8). The straight line connecting the the points $[1, V(1)]$ and $[2, V(2)]$ of graph single-well potential sets its convex hull.

thermostat with temperature T_- . The corresponding system of equations of motion of the chain can be written as

$$\begin{aligned} \ddot{u}_n &= -\partial H/\partial u_n - \gamma \dot{u}_n + \xi_n^+, & n \leq N_+, \\ \ddot{u}_n &= -\partial H/\partial u_n, & N_+ < n \leq N_+ + N, \\ \ddot{u}_n &= -\partial H/\partial u_n - \gamma \dot{u}_n + \xi_n^-, & n > N_+ + N, \end{aligned} \quad (3)$$

where $\gamma = 0.1$ is a relaxation coefficient, ξ_n^\pm models a white Gaussian noise normalized by the conditions $\langle \xi_n^\pm(t) \rangle = 0$, $\langle \xi_n^+(t_1) \xi_k^-(t_2) \rangle = 0$, and $\langle \xi_n^\pm(t_1) \xi_k^\pm(t_2) \rangle = 2\gamma T_\pm \delta_{nk} \delta(t_2 - t_1)$.

The system of equations of motion (3) was integrated numerically. Considered a chain with fixed ends: $u_1 \equiv 0$, $u_N \equiv (N - 1)a$. Used on-initial condition

$$\{u_n(0) = (n - 1)a, \dot{u}_n(0) = 0\}_{n=1}^{N_+ + N + N_-},$$

where $1 \leq a \leq 2$ —average value of the chain link length. After an initial transient, thermal equilibrium with the thermostats was established and a stationary heat flux along the chain appeared. A local temperature is numerically defined as $T_n = \langle \dot{u}_n^2 \rangle_t$ and the local heat flux—as $J_n = \bar{a} \langle j_n \rangle_t$, where $j_n = -\dot{u}_n V'(u_n - u_{n-1})$. In numerical simulations we used the following values of temperature $T_\pm = (1 \pm 0.1)T$ ($T = 0.01, 0.03, 0.1$), the relaxation coefficient $\gamma = 0.1$, the number of units $N_\pm = 40$, $N = 20, 40, 80, \dots, 10240$.

This method of thermalization overcomes the problem of the thermal boundary resistance. The distribution of the heat flow J_n and the temperature in the chain T_n (Fig. 2) clearly demonstrates that inside the “internal” fragment of the chain $N_+ < n \leq N_+ + N$ we observe a heat flux independent on the chain site, as one would expect in an energy-conserving system. Temperature profile also is almost linear. Thus, from this simulation one can unambiguously define the heat conduction coefficient of the internal chain fragment:

$$\kappa(N) = J(N - 1)/(T_{N_++1} - T_{N_++N}). \quad (4)$$

In the thermodynamical limit, one can say that the system obeys the Fourier law, if there exists a finite limit

$$\bar{\kappa} = \lim_{N \rightarrow \infty} \kappa(N).$$

If such a limit does exist, one can say that the chain has normal (finite) or convergent heat conduction. In the opposite case, an anomalous heat conduction is observed.

An alternative way for evaluation of the heat conduction coefficient is based on linear response theory, which leads, in particular, to the famous Green-Kubo expression [29],

$$\kappa_c = \lim_{t \rightarrow \infty} \lim_{N \rightarrow \infty} \frac{1}{NT^2} \int_0^t c(\tau) d\tau, \quad (5)$$

where the autocorrelation function of the heat flux in the chain is defined as $c(t) = \langle J_s(\tau) J_s(\tau - t) \rangle_\tau$. Here a total heat flux in the chain is defined as $J_s(t) = \sum_n j_n(t)$.

In order to compute the self-correlation function $c(t)$ we simulate a cyclic chain consisting of $N = 10^4$ particles and couple all these particles to the Langevin thermostat with temperature T . After initial thermalization, the chain has been detached from the thermostat and Hamiltonian dynamics has been simulated. In order to improve the accuracy, the self-correlation function has been computed by averaging over 10^4

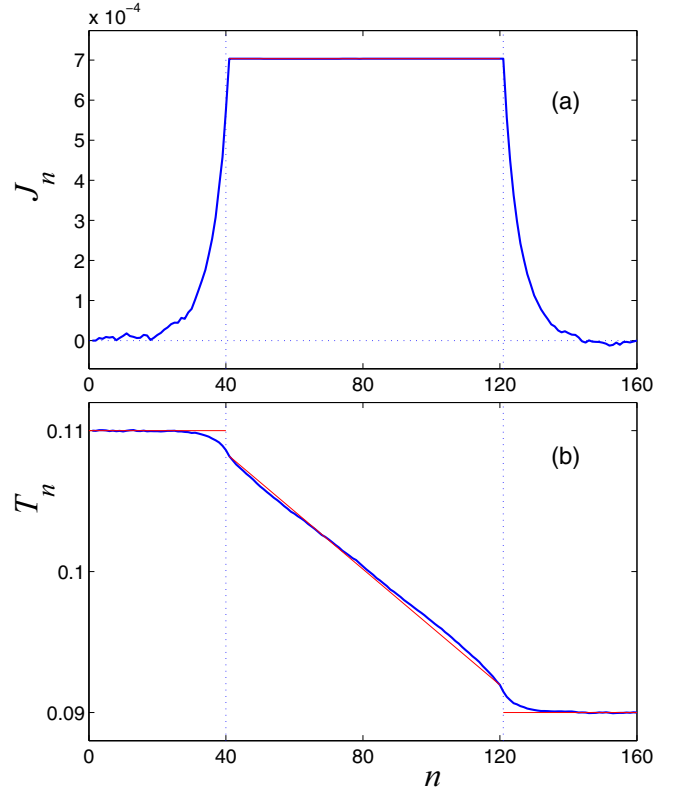


FIG. 2. (Color online) Profile of (a) local heat flux J_n and (b) local temperature T_n in the chain with DW potential Eq. (2) for $N_\pm = 40$, $N = 80$, $T_+ = 0.11$, $T_- = 0.09$. Linear approximation of the temperature distribution (thin red line) is used for evaluation of the heat-conduction coefficient $\kappa(N)$.

realizations with independent initial conditions, corresponding to the same initial temperature T .

The heat conduction turns out to be convergent if the self-correlation function $c(\tau)$ decreases fast enough as $\tau \rightarrow \infty$. Namely, if the integral in Eq. (5) converges then the heat conduction may be treated as normal.

III. CHAIN WITH SYMMETRIC DW POTENTIAL

First, we explore thermodynamical properties of the DW chain in thermal equilibrium. For this sake, in Fig. 3 we present a dependence of heat capacity of the chain (defined as $C_v = dE/dT$ for fixed length of the chain) on the average temperature for three different values of the interatomic distance. We observe that all these dependencies exhibit a hump in a region of low temperatures—below the value of potential barrier. This hump characterizes the state where the potential has the strongest effect on the chain dynamics. For the case with the largest number of competing ground states, $a = 1.5$, the hump is the most pronounced. It means that in this case one should expect the strongest nonlinear scattering, in good correlation with further findings.

Dependence of the heat-conduction coefficient κ on the length of the chain fragment between the Langevin thermostats N for the chain with symmetric DW potential Eq. (2) is presented in Fig. 4. As one can see from this figure,

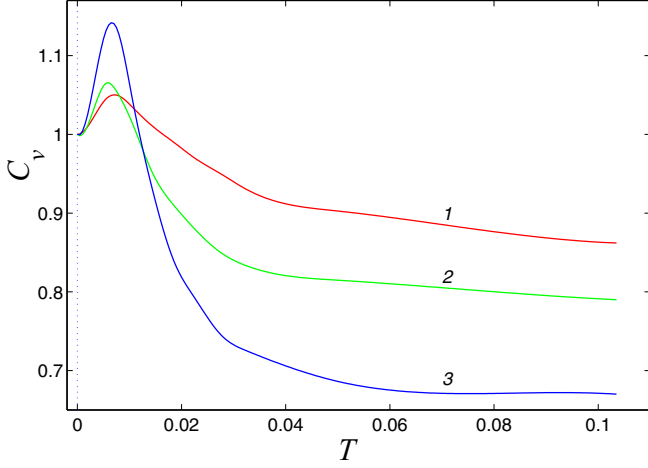


FIG. 3. (Color online) Dependence of the heat capacity of the chain C_v with DW potential Eq. (2) on the temperature T for the average interatomic distances $a = 1, a = 1.1$, and $a = 1.5$ (curves 1, 2, 3, respectively).

both for $a = 1$ and $a = 1.5$ the heat conduction coefficient grow monotonously with N and demonstrates no trend for

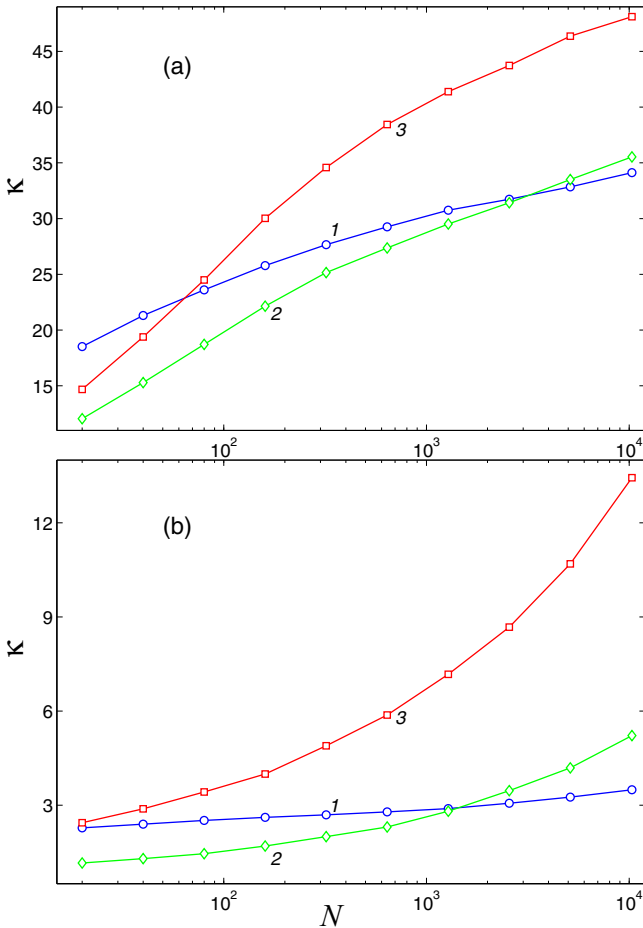


FIG. 4. (Color online) Dependence of the heat conduction coefficient κ on the size of the internal chain fragment N for the chain with the DW potential Eq. (2) for the average interatomic distance (a) $a = 1$ and (b) $a = 1.5$ for temperatures $T = 0.01, 0.03, 0.1$ (curves 1, 2, 3, respectively).

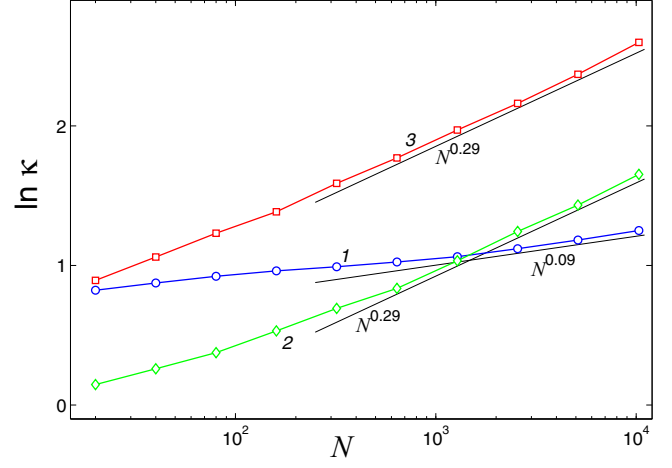


FIG. 5. (Color online) Dependence of the heat conduction coefficient κ on the size of the internal chain fragment N for the chain with the DW potential Eq. (2) for the average interatomic distance $a = 1.5$ for temperatures $T = 0.01, 0.03, 0.1$ (curves 1, 2, 3, respectively). The graphs are presented in double logarithmic scale and straight lines correspond to fitting N^α , $\alpha = 0.09, 0.29, 0.29$, for curves 1, 2, 3, respectively.

convergence. For $a = 1.5$ the heat conduction coefficient grows like N^α , with $\alpha = 0.09$ for the temperature $T = 0.01$ and $\alpha = 0.29$ for $T = 0.03, 0.1$, as is demonstrated in Fig. 5.

Numeric analysis of the heat-flux autocorrelation function $c(t)$ as $t \rightarrow \infty$ supports the conclusion on divergent heat conductivity in the system. For all values of the average link length $1 \leq a \leq 2$ the function $c(t)$ decreases as $t \rightarrow \infty$ according to the power law $t^{-\beta}$ with exponent $\beta < 1$, as it is demonstrated in Fig. 6. According to the Green-Kubo formula, Eq. (5), one arrives to the same conclusion on divergence of the heat-conduction coefficient $\kappa(N)$ as $N \rightarrow \infty$. Two approaches used here are independent and point in the same direction—one obtains clear indication that the heat conductivity in the chain with DW potential diverges.

So, as it was already mentioned in the Introduction, it is reasonable to explore and compare the heat-conduction coefficient $\kappa(N)$ for some fixed chain length. To be specific, we choose $N = 640$ and consider the temperature dependence of the heat conductivity for fixed number of particles and varying average link length. The results are presented in Fig. 7. For all presented values of the link length the heat conductivity in the case of low temperatures $T < 0.01$ sharply decreases as the temperature grows. For large temperatures the heat conductivity weakly increases with the temperature. In all cases the minimum is achieved in the temperature interval $0.01 \div 0.04$, which is close to the height of the potential barrier. The lowest values of the heat-conduction coefficient are obtained for $a = 1.5$. This result is expectable, since namely for this value of the average link length the number of topologically different degenerate ground states achieves a maximum.

From Fig. 7 one can see that if the average link length a varies from 1 to 1.5, the heat-conduction coefficient decreases monotonously. In order to estimate the efficiency of the heat-conductivity reduction, we define the reduction

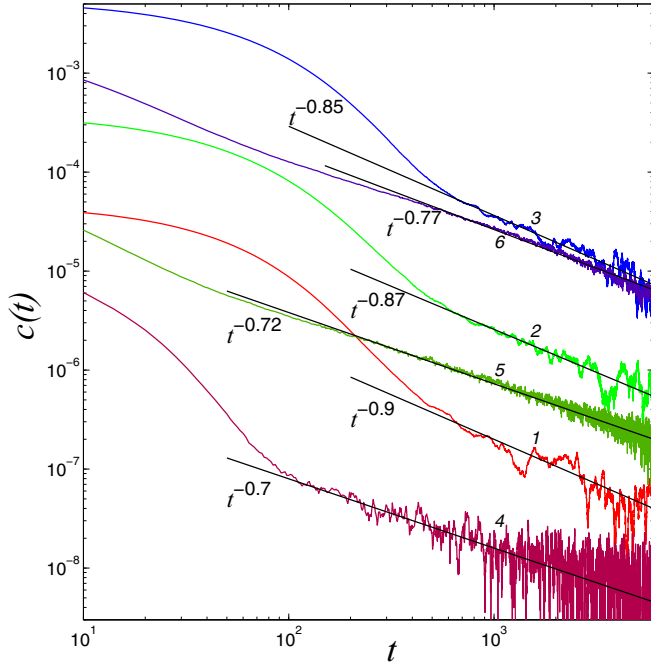


FIG. 6. (Color online) Power-law decrease of the autocorrelation function $c(t)$ for the chain with symmetric DW potential Eq. (2) for average link length $a = 1$ and temperatures $T = 0.01, 0.03, 0.1$ (curves 1, 2, 3, respectively) and $a = 1.5, T = 0.01, 0.03, 0.1$ (curves 4, 5, 6, respectively). The graphs are presented in double logarithmic scale and straight lines correspond to fitting $t^{-\beta}$, $\beta = 0.9, 0.87, 0.85, 0.7, 0.72, 0.77$ for curves 1, 2, ..., 6, respectively.

coefficient $\mu_a = \kappa(a, N, T) / \kappa(1, N, T)$, where $\kappa(a, N, T)$ denotes the heat-conduction coefficient for the average link length a , number of particles N and temperature T . We note that by symmetry considerations it is enough to consider only the interval $1 \leq a \leq 1.5$.

A dependence of μ_a on the temperature and the average link length is presented in Fig. 8. The heat conductivity decreases with increase of a for all studied values of the

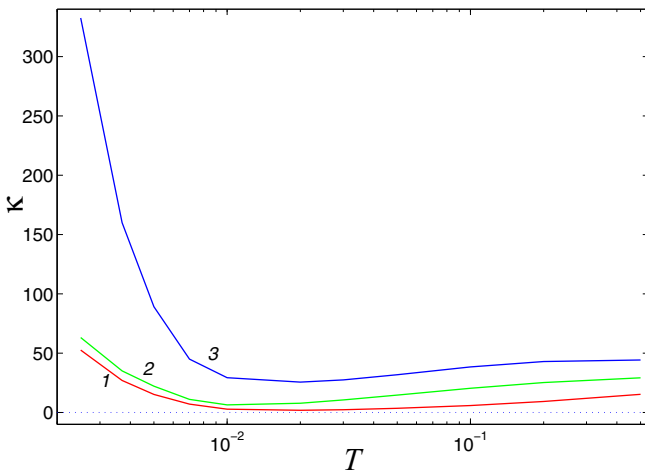


FIG. 7. (Color online) Dependence of the heat conduction coefficient κ on temperature T of the chain containing in general 720 particles ($N = 640, N_{\pm} = 40$) with the DW potential Eq. (2) for $a = 1.5, 1.1, 1.0$ (curves 1, 2, 3, respectively).

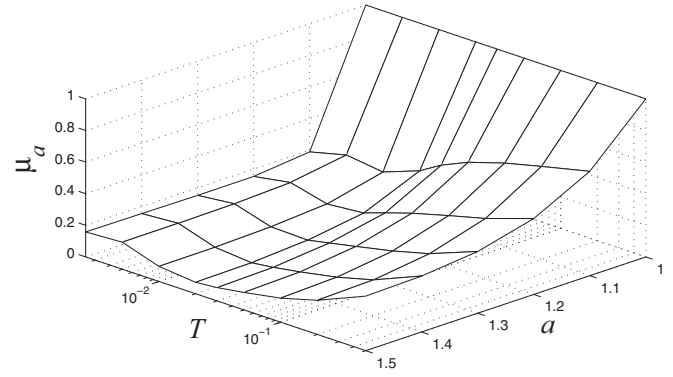


FIG. 8. Dependence of the reduction coefficient of heat conductivity $\mu_a = \kappa(a) / \kappa(1)$ on the temperature T and the average link length a [$\kappa(a)$ —heat conductivity of the chain with the average link length a].

temperature. Maximal efficiency of the reduction is achieved for the temperature $T = 0.02$, which is close to the height of the potential barrier $E_0 = 0.0313$. As one could expect, maximal reduction of the heat conductivity occurs at $a = 1.5$.

However, other aspect of the reduction phenomenon is somewhat unexpected. In Fig. 9 we present the dependence of the reduction efficiency for different temperatures $\mu_N = \kappa(1.5, N, T) / \kappa(1, N, T)$ as a function of the particle number N . It is somewhat surprising to see that this dependence is not monotonous. The chain length for which the most efficient reduction of the heat conductivity is observed strongly depends on the temperature. For instance, for $T = 0.01$ the most efficient reduction is observed when $N_0 = 1280$, and for higher temperatures $T = 0.03, 0.1$ —when $N_0 = 160$.

It is easy to explain why for relatively short chains the reduction efficiency is higher when the chain gets longer. We believe that the reduction of the heat conductivity occurs due to increase of a number of the degenerate ground states.

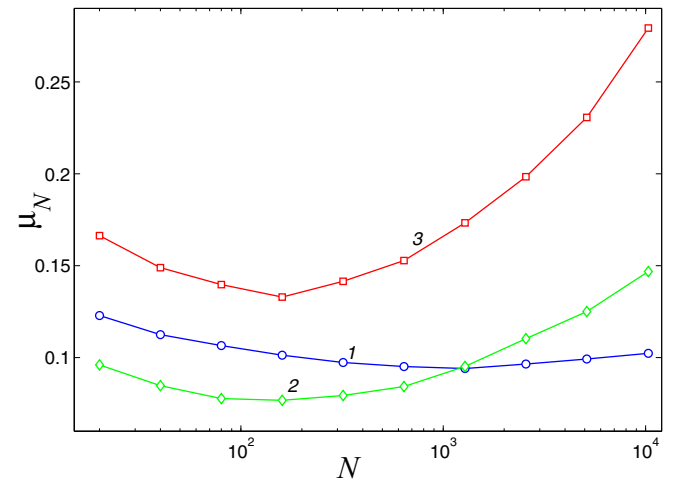


FIG. 9. (Color online) Dependence of the reduction coefficient of heat conductivity $\mu_N = \kappa(1.5) / \kappa(1)$ on the chain length N for temperature values $T = 0.01, 0.03, 0.1$ (curves 1, 2, 3, respectively). Here $\kappa(a)$ is heat conductivity of the chain with average link length a .

Quite obviously, this effect becomes more profound as the number of particles grows. The decrease of the reduction efficiency for relatively high N is more difficult to explain. Qualitatively, one can speculate that, since the heat-conduction coefficient in the chain with DW potential diverges, for very large N the heat transfer is governed by long-wavelength weakly interacting phonons. Such waves are less sensitive to the details of the chain structure and “feel” only average density of the particles.

It is also instructive to compare the process of nonstationary heat conduction in the DW model with different average link length. For this sake, following a methodology developed in Refs. [33,34], we simulate a relaxation of various spatial modes of a thermal perturbation in the cyclic DW chain with N particles. Thus, the initial temperature distribution is defined according to the following relationship:

$$T_n = T_0 + A \cos[2\pi(n-1)/Z], \quad (6)$$

where T_0 is the average temperature, A is the amplitude of the perturbation, and Z is the length of the mode (number of particles). The overall number of particles N has to be a multiple of Z in order to ensure the periodic boundary conditions.

In order to realize this initial thermal perturbation, each particle in the chain is first attached to a separate Langevin thermostat. In other terms, we integrate numerically the following system of equations:

$$\ddot{u}_n = -\partial H/\partial u_n - \gamma \dot{u}_n + \xi_n, \quad (7)$$

where $n = 1, 2, \dots, N$, $\gamma = 0.1$, and the action of the thermostat is simulated as white Gaussian noise normalized according to conditions

$$\langle \xi_n(t_1) \xi_k(t_2) \rangle = 2\gamma T_n \delta_{kn} \delta(t_2 - t_1).$$

After the initial heating in accordance with Eq. (6), the Langevin thermostat is removed and relaxation of the system to a stationary temperature profile is explored. The results were averaged over 10^6 realizations of the initial profile $\{T_n\}_{n=1}^N$ in order to reduce the effect of fluctuations.

Samples of the nonstationary simulations are presented in Figs. 10 and 11. In both figures, we compare the relaxation of similar thermal perturbation profiles with similar average temperature, perturbation amplitude, and spatial wavelength. The only difference is the average link length. We compare the two extreme cases $a = 1$ and $a = 1.5$. In Fig. 11 one can see that the same thermal perturbation for $a = 1$ decays in oscillatory manner, whereas for $a = 1.5$ the decay is smooth. Thus, one can conclude that for the case $a = 1$ the relaxation cannot be reliably described by common diffusion equation. In such cases, higher-order corrections are invoked and the thermal relaxation may be described by equations of hyperbolic type, like, e.g., the Cattaneo-Vernotte equation [33,34]. In the same time, for the case $a = 1.5$ one observes primarily diffusive behavior. This conclusion is further confirmed by simulation results presented in Fig. 10. There we can see that for $a = 1$ the oscillatory behavior is observed for very broad diapason of the wavelengths. For all these modes, the thermal perturbations for $a = 1.5$ decay in a primarily diffusive manner. The reason for this difference, again, is a

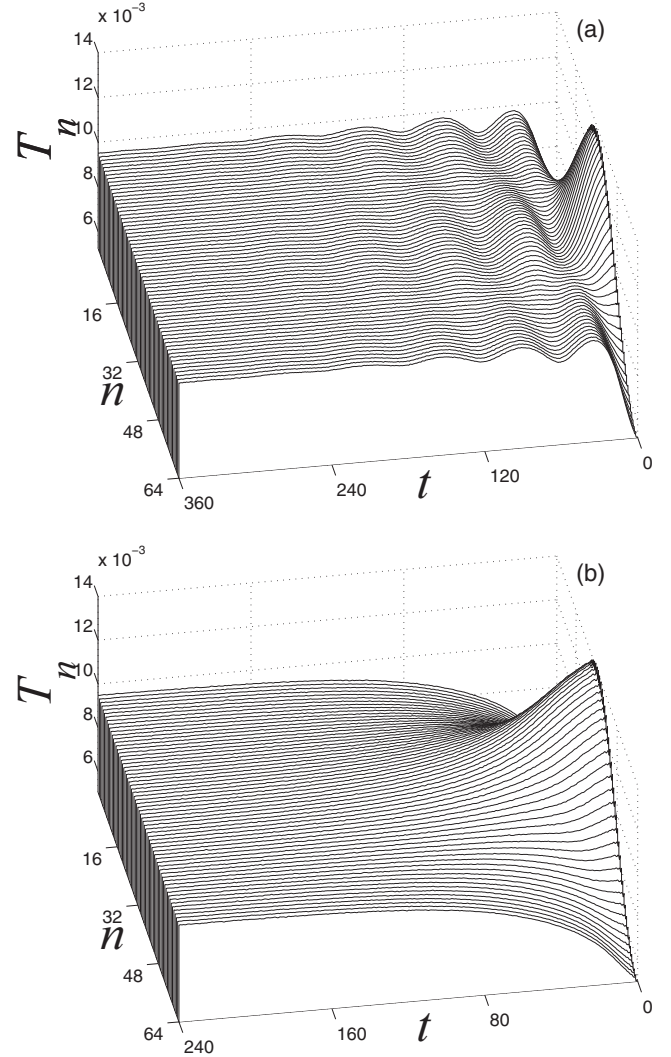


FIG. 10. Relaxation of initial periodic thermal profile in the periodic chain with potential Eq. (2) $N = 1024$, $T_0 = 0.01$, $A = 0.05$, $Z = 64$ for (a) $a = 1$ and (b) $a = 1.5$.

“perfect” structure of the ground state for $a = 1$ and large number of the degenerate ground states for $a = 1.5$.

IV. A MODEL WITH NONCONVEX SINGLE-WELL POTENTIAL

The results presented in the previous section suggest that the increase of the number of the ground states peculiar for the DW chain leads to suppression of the heat conduction. One should expect even stronger suppression effect, when the chain is modified in a way that the potential changes from single-well to double-well. Possibility of such modification in a particular chain model under action of an external force and the consequences for the heat conductivity are discussed here. First of all, we suggest a model of the chain with a nonconvex single-well potential of the nearest-neighbor interaction:

$$V(\rho) = \epsilon(\rho - 1)^2(\rho - 2)^2 + \beta\rho + c, \quad (8)$$

where $\epsilon = 1/2$, $\beta = 0.15$, and (physically insignificant) constant c may be found from a condition $\min V(\rho) = 0$.

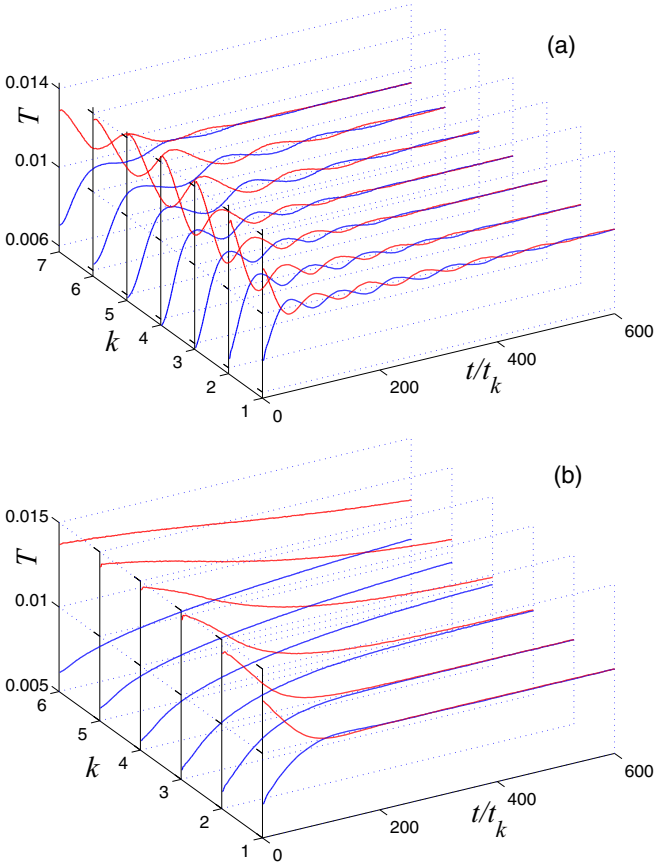


FIG. 11. (Color online) Evolution of the relaxation profile in the periodic chain with double-well potential Eq. (2) ($N = 2048$, $T_0 = 0.01$, $A = 0.05$) for (a) $a = 1$ ($Z = 2^{3+k}$, $k = 1, 2, \dots, 7$, $t_k = 0.15$, $0.3, 0.6, 1.2, 2.0, 4.0, 10.0$) and (b) $a = 1.5$ ($Z = 2^{3+k}$, $t_k = 0.1 \times 2^{k-1}$, $k = 1, 2, \dots, 6$). Time dependence of the mode maximum $T(1 + Z/2)$ [red (gray) lines] and minimum $T(1)$ [blue (black) lines] are depicted.

Under these values of parameters potential function Eq. (8) has a single minimum at $\rho_0 = 0.89$ (Fig. 1).

Let us consider the case when the chain with potential Eq. (8) is elongated by external force F applied to one of its ends, whereas the other end remains fixed. It is easy to see that such external forcing is equivalent to a modification of the interaction potential Eq. (8) while adding a linear term with negative slope. This modified potential will have the following form:

$$V^*(\rho) = \epsilon(\rho - 1)^2(\rho - 2)^2 + \beta\rho - F\rho + c. \quad (9)$$

Thus, the application of the external force can modify the topology of the potential function. Namely, it is easy to demonstrate that for $F < F_{\min} = \beta - \epsilon/3\sqrt{3}$ and for $F > F_{\max} = \beta + \epsilon/3\sqrt{3}$ the potential $V^*(\rho)$ remains single-well. However, for $F_{\min} < F < F_{\max}$ the effective potential becomes double-well, and thus one can expect significant reduction of the heat conductivity as a result of application of the external force.

In our numeric experiments we control the average link length a rather than the value of the external force. However, it is easy to translate between these quantities. Namely, potential function Eq. (9) will have two wells if the following condition

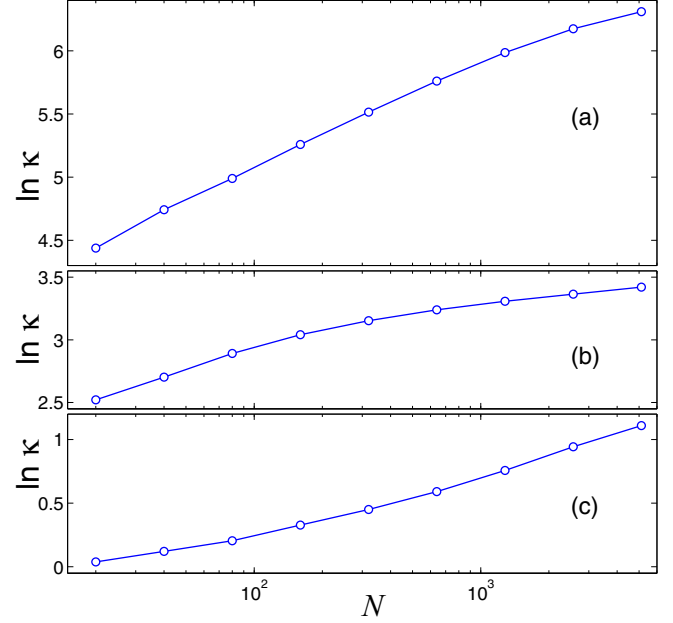


FIG. 12. (Color online) Dependence of heat-conduction coefficient κ on the chain length N for the chain with single-well nearest-neighbor potential Eq. (8) for different values of the average link length: (a) $a = \rho_0$, (b) $a = 2.0$, (c) $a = 1.5$. In all cases the temperature $T = 0.01$.

holds: $a_{\min} < a < a_{\max}$, where $a_{\min} = 3/2 - 1/\sqrt{3} \approx 0.9226$ and $a_{\max} = 3/2 + 1/\sqrt{3} \approx 2.0774$.

Creation of the effective double-well potential can be also explained from observation of the single-well potential function Eq. (8) depicted in Fig. 1. One can see that this function is not convex (the second derivative is negative for $1 \leq \rho \leq 2$). Homogeneous extension of such a chain, when all the links have the same length $\rho_n \equiv a > \rho_0$, is energetically favorable only when the average link length belongs to the interval where the potential function coincides with its convex hull: $a \leq \rho_1 = 1$ and $a \geq \rho_2 = 2$. If $\rho_1 < a < \rho_2$, it is more favorable to have part of the links with the length $\rho_n \equiv \rho_1 = 1$, and the rest—with the length $\rho_n \equiv \rho_2 = 2$. In this case, the dependence of the average potential energy per particle on the average link length will follow the straight line connecting the points $[\rho_1, V(\rho_1)]$ and $[\rho_2, V(\rho_2)]$, as it is demonstrated in Fig. 1 [35,36]. Thus, as the average link length increases, the numbers of “short” and “long” links vary accordingly, thus giving rise to a large number of possible realizations and large variations of the heat conduction coefficient.

Heat transfer in this system has been simulated with the help of Langevin thermostats Eq. (3) under fixed-ends boundary conditions: $u_1(t) \equiv 0$, $u_{N_+ + N + N_-} = (N_+ + N + N_- - 1)a$, where again $a \geq \rho_0$ is the average length of the link.

Numeric simulation of the heat conduction demonstrated that for all studied values of the average link length $a \geq \rho_0$, the heat-conduction coefficient diverges: $\kappa(N) \nearrow \infty$ as $N \nearrow \infty$ —see Fig. 12. Equilibrium simulations based on Green-Kubo formula Eq. (5) bring about the same conclusion.

The dependence of the heat-conduction coefficient κ on the average link length a for the chain with the single-well nonconvex potential of the nearest-neighbor interaction Eq. (8)

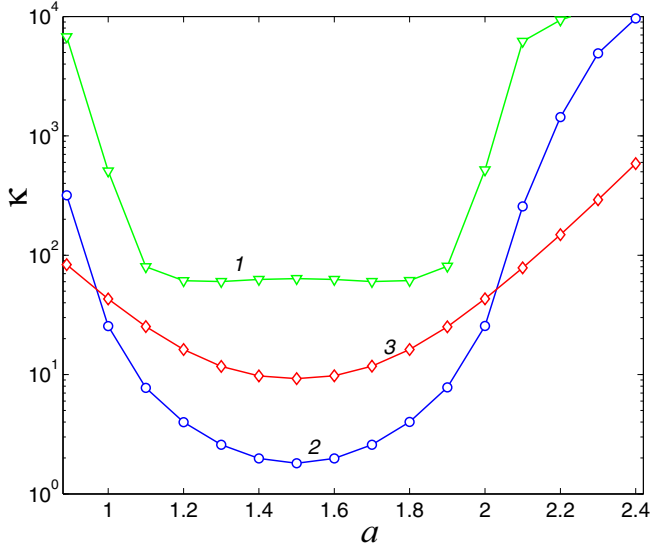


FIG. 13. (Color online) Dependence of the heat conduction coefficient κ in the chain with single-well potential of the nearest-neighbor interaction Eq. (8) on the average link length a for temperatures $T = 0.002, 0.02, 0.2$ (curves 1, 2, 3, respectively). Note a logarithmic scale for κ . Simulated chain contained in all cases $N_+ + N + N_-$ particles, $N = 640$ of them were free and $N_{\pm} = 40$ were immersed in the Langevin thermostats with temperatures $T_{\pm} = (1 \pm 0.1)T$.

is presented in Fig. 13. One can observe very strong effect of the chain extension on the heat-conduction coefficient. This drastic reduction is observed for values of the average link length approximately in the interval $1 < a < 2$, in accordance with earlier findings on the relationship between a number of possible degenerate (or close energetically) ground states and the reduction of the heat conductivity.

It is possible to say that these drastic modifications of the heat-conduction coefficient occur due to “latent” double-well nature of the nonconvex potential of the nearest-neighbor interaction. Notably, the most efficient reduction is achieved when the temperature is close to the height ϵ of the “latent” potential barrier. The reduction of the heat conductivity by two orders of magnitude is achieved for $T = 0.02$.

It is important to mention that the effective nonconvex single-well potential is obtained in effective models of some quasi-one-dimensional objects. For instance, it is realized in α spirals of protein macromolecules, double helix of DNA [35,36], as well as in a model of intermetallic NiAl crystalline nanofilms [37]. In these structures the external extension brings nonhomogeneous equilibrium configurations. Then, one should expect strong effect of external mechanic loads on transport properties in systems of this sort.

V. CONTROL OF THE HEAT TRANSPORT IN MODELS WITH CONVERGENT HEAT CONDUCTION

All simple models considered above are believed to have the divergent heat conductivity in the thermodynamical limit. In this section, we are going to consider a modification of chain of rotators, which allows external control of the heat-conduction coefficient. Simple chain of rotators is believed to exhibit convergent heat conductivity [20,21].

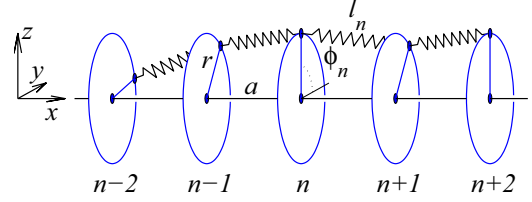


FIG. 14. (Color online) Sketch of the modified chain of rotators.

To explain the idea of possible modification, let us consider a mechanical model sketched in Fig. 14—a chain of equal parallel disks of radius r with centers fixed at equal intervals of length a along x axis. The disks can rotate along the x axis and the rotation angle of the n th disk is denoted as ϕ_n . Neighboring disks are coupled by harmonic springs of equal stiffness and equilibrium length. The Hamiltonian of such a model can be simply expressed as follows:

$$H = \sum_{n=1}^N \frac{1}{2} I \dot{\phi}_n^2 + V(\phi_{n+1} - \phi_n), \quad (10)$$

where I is a moment of inertia of the disk. Potential energy of relative rotation appears due to deformation of the springs, which couple the neighboring disks, and is expressed as

$$V(\Delta\phi_n) = \frac{1}{2} K (l_n - L_0)^2 = \frac{1}{2} K \{ [a^2 + 2r^2(1 - \cos(\Delta\phi_n))]^{1/2} - L_0 \}^2. \quad (11)$$

Here, $\Delta\phi_n = \phi_{n+1} - \phi_n$ is a relative rotation angle of the neighboring disks, K and L_0 are the stiffness and equilibrium length of the springs, respectively, and l_n is the length of the n th spring. Potential function Eq. (11) will be double-well provided that $a < L_0 < [a^2 + 4r^2]^{1/2}$. The potential minima in this case correspond to the following values of the relative rotation angle:

$$\Delta\phi_0 = \pm 2 \arcsin \{ [(L_0^2 - a^2)/4r^2]^{1/2} \}.$$

The characteristic shape of the modified potential function Eq. (11) is presented in Fig. 15. Without affecting the generality, one can set $I = 1$, $a = 1$, and $K = 1$. To be specific, we also choose $r = 1$. Thus, the potential will have two wells for the equilibrium length of the spring in the interval $1 < L_0 < \sqrt{5}$. The function $V(\Delta\phi)$ is 2π -periodic and has two potential barriers $0 < \epsilon_0 < \epsilon_1$. If the equilibrium spring length L_0 will only slightly exceed the distance a between the disk centers, then one will obtain $\epsilon_0 \ll \epsilon_1$. For instance, for $L_0 = 1.2$ one obtains the potential minima $\Delta\phi_0 = \pm 0.2152\pi \approx 0.6761$, and the barriers $\epsilon_0 = 0.02$, $\epsilon_1 = 0.5367$.

We expect that, similar to the simple chain of dipole rotators [20,21], the chain with Hamiltonian Eq. (10) will have converging heat conduction coefficient.

To simulate the heat conductivity, we attach the chain ends with $N_{\pm} = 40$ disks to Langevin thermostats with temperatures $T_{\pm} = (1 \pm 0.1)T$. Then, we simulate numerically the system of Eq. (3) with potential function obtained from Eq. (11) under fixed boundary conditions $\varphi_0 \equiv 0$, $\varphi_M \equiv (N_+ + N + N_- - 1)\varphi_0$ and with initial conditions

$$\{\varphi_n(0) = (n-1)\varphi_0, \dot{\varphi}_n(0) = 0\}_{n=1}^{N_+ + N + N_-},$$

where φ_0 —average value of angle between neighboring disks. In other terms, we keep constant relative rotation angle

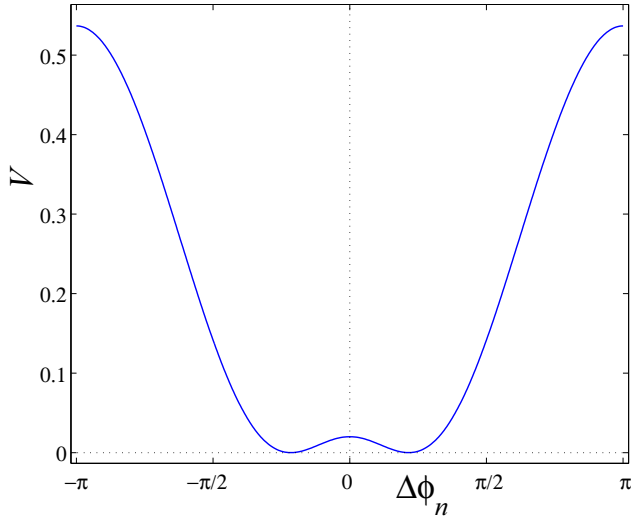


FIG. 15. (Color online) Shape of potential function Eq. (11) $V(\Delta\phi)$ for $a = 1$, $r = 1$, $L_0 = 1.2$, $K = 1$. Heights of the potential barriers are $\epsilon_0 = 0.02$, $\epsilon_1 = 0.5367$. The potential function achieves the minima for $\Delta\phi = \pm 0.2152\pi$.

between the ends of the chain (in other terms, we apply constant momentum to the chain) and study the dependence of the heat conduction coefficient on these external conditions.

Dependence of the heat-conduction coefficient κ on the length of the chain fragment between the Langevin thermostats N for the chain with periodic potential Eq. (11) is presented in Fig. 16. As one can see, the value of N for which the heat conductivity converges strongly depends on the average temperature T .

For average temperature $T = 0.2$ comparable to a value of the higher potential barrier ϵ_1 , the convergence is reliably achieved already for $N = 320$. We also see that the heat

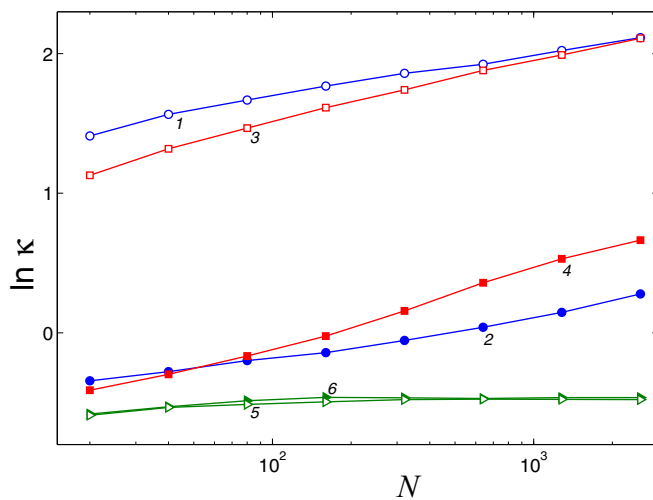


FIG. 16. (Color online) Dependence of the heat conduction coefficient κ on the size of the internal chain fragment N for the chain with periodic potential Eq. (11) for the average angle between the disks $\varphi_0 = \Delta\phi_0$ and $\varphi_0 = 0$, respectively (curves 1 and 2 for temperature $T=0.01$, curves 3 and 4—for $T = 0.02$, curves 5 and 6—for $T = 0.2$).

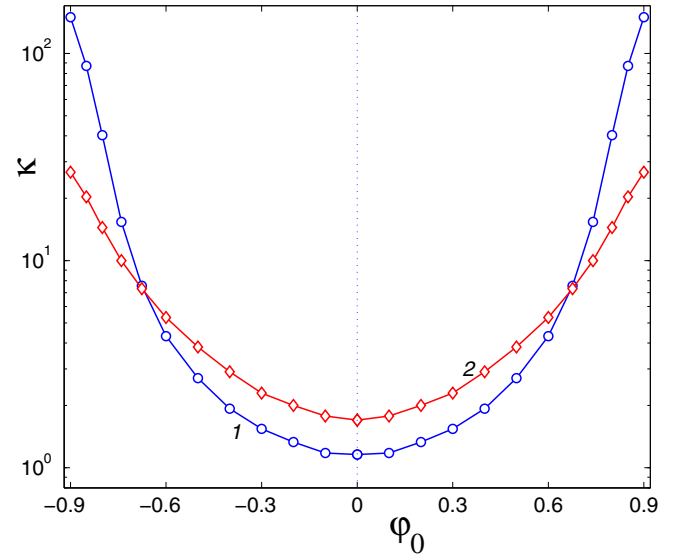


FIG. 17. (Color online) Dependence of the heat conduction coefficient κ in the chain with periodic potential of the nearest-neighbor interaction Eq. (11) on the average interdipole angle φ_0 for temperatures $T = 0.01, 0.02$ (curves 1, 2, respectively).

conduction coefficient almost does not depend on φ_0 . The latter result seems natural, since the temperature is large enough to allow frequent transitions over the higher barrier; then, the initial mutual rotation of the disks is relaxed.

If the average temperature will be much lower than the higher potential barrier $T \ll \epsilon_1$, the relaxation mentioned above will require exponentially large time. In this case, the heat conduction still converges, but the convergence requires consideration of much larger values of the chain length N . For every chain length, the heat conductivity in the chains with $\varphi_0 = 0$ is significantly higher than in the chains with $\varphi_0 = \Delta\phi_0$. For the average temperature $T = 0.01$, the difference is 6.5 times, and for $T = 0.02$, 5 times.

To check this assumption further, let us consider also the dependence of κ on the initial angle between the disks φ_0 for the chain length $N = 1280$. In Fig. 17, one can clearly observe that this dependence is strong enough, provided that the temperature is sufficiently low to prevent the fast relaxation.

Physical reasons of this behavior are very similar to those described in the preceding sections. For $|\varphi_0| \leq \Delta\phi_0$ the chain has energetically degenerate ground states, where part of the neighboring disk pairs have relative equilibrium angle $\phi_{n+1} - \phi_n = \Delta\phi_0$, and the other pairs, $\phi_{n+1} - \phi_n = -\Delta\phi_0$. A number of possible different ground states grows as $|\varphi_0|$ tends to zero. That is why the heat conductivity decreases in this limit. This effect becomes more pronounced as the temperature decreases. Still, for extremely small temperatures the heat conductivity will cease to depend on $|\varphi_0|$, since even the smaller potential barriers will become prohibitive.

For exponentially large simulation times the dependence of the heat conductivity on the initial relative rotation of the disks is expected to disappear due to thermally activated relaxation over higher potential barriers. In our simulations the times were not large enough to observe this relaxation for lower temperatures. Still, we believe that this problem may be easily

overcome. It seems sufficient to act with constant external momentum on the right end of the chain, rather than to fix it. Then, one should investigate a dependence of the heat conduction coefficient on the value of this external momentum.

The idea presented in this section could be useful for practical design of the systems with controlled heat conductivity. One can use, for instance, the stretched polymer macromolecules. Thermal conductivity in such polymers is studied rather widely [38,39]. We conjecture that in polymers with large size groups the heat conductivity can be modified by application of the external momentum.

VI. HEAT CONDUCTION IN STRETCHED α HELIX

Above we restricted ourselves to one-dimensional models. In this section we are going to demonstrate that the mechanical control of the heat transport may be achieved also in a model of three-dimensional molecular helix. For this sake we consider a 3D molecular chain describing an ideal α helix.

Particles comprising this helix in the state of equilibrium have the following Cartesian coordinates:

$$\mathbf{R}_n^0 = [R_0 \cos(n\phi_0), R_0 \sin(n\phi_0), n\Delta z_0], \quad (12)$$

where $n = 0, \pm 1, \pm 2, \dots$ are numbers of the helix particles, R_0 is a radius of the helix, and ϕ_0 and Δz_0 are angular and translational periods of the helix, respectively. Such a helix can be treated as a quasi-1D crystal; that is, each site can be obtained from the previous one by the appropriate translation along longitudinal axis z and rotation around the same axis.

Hamiltonian of the chain is expressed as

$$H = \sum_n \left\{ \frac{1}{2} M (\dot{\mathbf{R}}_n, \dot{\mathbf{R}}_n) + V(\rho_n) + U(\theta_n) + W(r_n) \right\}. \quad (13)$$

Here, $\mathbf{R}_n(t) = (R_{n,1}, R_{n,2}, R_{n,3})$ is a 3D vector denoting a position of the n th particle (peptide group) of the helix at time instance t , and M is a mass of the particle. Potential $V(\rho_n)$ corresponds to the energy of the nearest-neighbor interaction, $\rho_n = |\mathbf{u}_n|$, $\mathbf{u}_n = \mathbf{R}_{n+1} - \mathbf{R}_n$. Energy of deformation of planar valence angles is described through the term $U(\theta_n)$, where θ_n corresponds to a value of the valence angle centered at particle n , $\cos(\theta_n) = -(\mathbf{u}_{n-1}, \mathbf{u}_n) / \rho_{n-1} \rho_n$. The last term in the Hamiltonian, $W(r_n)$, describes a deformation energy of the n th hydrogen bond, coupling between the n th and $n+3$ rd particles, $r_n = |\mathbf{R}_{n+3} - \mathbf{R}_n|$.

For the sake of simplicity we consider a reduced dimensionless model of the helix with $M = 1$, equilibrium interparticle distance $\rho_0 = 1$, angular equilibrium step of the helix $\phi_0 = 100^\circ$, and equilibrium valence angle $\theta_0 = \arccos(-1/3) = 109.47^\circ$. Then [40], the nondimensional helix radius should be

$$R_0 = \rho_0 \cos(\theta_0/2) / [1 - \cos(\phi_0)] = 0.4919,$$

and the step along the axis is

$$\Delta z_0 = \rho_0 \sqrt{|\cos(\phi_0) + \cos(\theta_0)| / [1 - \cos(\phi_0)]} = 0.6572,$$

and the equilibrium length of the hydrogen bond is $r_0 = 2.0322$.

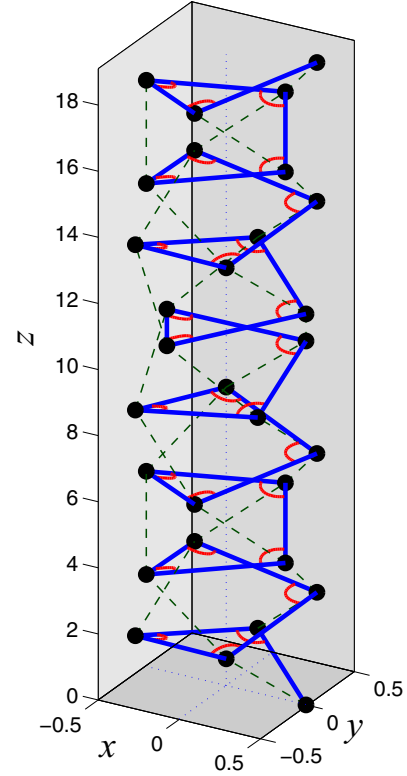


FIG. 18. (Color online) Sketch of the α helix in the state of equilibrium. Solid lines correspond to the valence bonds, arches to the valence angles, and dashed lines to the hydrogen bonds.

To be specific, we describe the deformation of the rigid valence bond by harmonic potential

$$V(\rho) = \frac{1}{2} K (\rho - \rho_0)^2, \quad (14)$$

with stiffness $K = 4$, deformation of the valence angle—by the potential

$$U(\theta) = \epsilon_1 (\cos \theta - \cos \theta_0)^2, \quad (15)$$

with characteristic energy $\epsilon_1 = 0.25$, and the hydrogen bond—by Morse potential

$$W(r) = \epsilon_0 \{ \exp[-\beta(r - r_0)] - 1 \}^2, \quad (16)$$

with parameters $\epsilon_0 = 0.005$, $\beta = 10$.

A sketch of the equilibrium state of the helix is presented in Fig. 18. Similar models were used before [40,41] for analysis of supersonic solitary waves. In Ref. [35] it was demonstrated that the homogeneous stretching of the helix leads to appearance of the effective nonconvex single-well potential. Minimization of potential energy in Eq. (13) for homogeneous growth of Δz leads to effective potential plotted in Fig. 19. As one can see, the equilibrium value of the angular step ϕ grows monotonously and for $\Delta z = 0.8181$ achieves the maximum possible value $\phi = 180^\circ$ —thus the helix is decoiled into a planar trans-zigzag.

As one can see from Fig. 19 the effective potential $E(\Delta z)$ is not convex. The convex envelope is obtained by attaching a line between points $[\Delta z_1, E(\Delta z_1)]$ and $[\Delta z_2, E(\Delta z_2)]$, where $\Delta z_1 = 0.6725$, $\Delta z_2 = 0.8254$. This line describes the scenario of nonhomogeneous stretching, where some segments of the

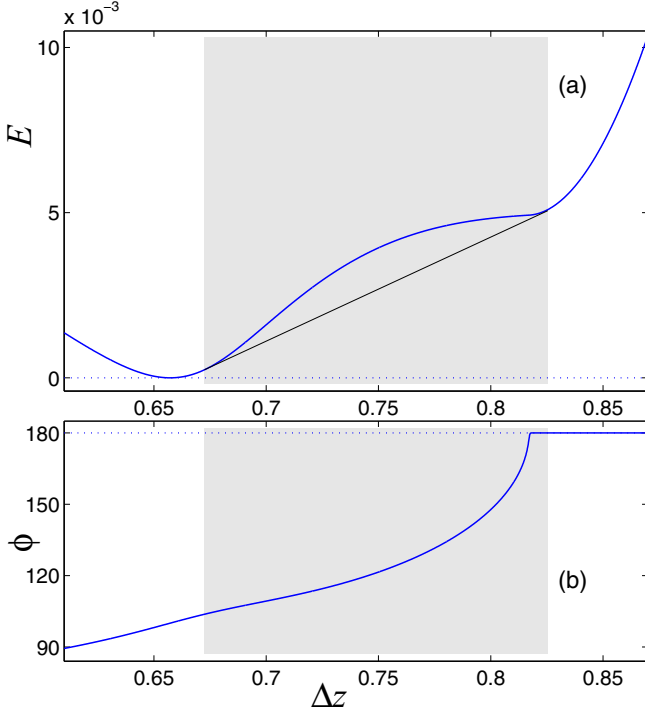


FIG. 19. (Color online) Dependence of (a) energy E and (b) angular step of the helix ϕ on its axial step Δz . Gray shadow denotes a region in which the nonhomogeneous stretching turns out to be energetically favorable.

helix are stretched weakly with the step Δz_1 and the others are stretched strongly, with the step Δz_2 . The stretching is achieved through growth of a number of the strongly stretched segments. Obviously, such a scenario is more favorable energetically than the homogeneous stretching.

To simulate the heat transfer in the helix chain, we used the protocol of equilibrium heat transfer between Langevin thermostats, similar to that used for the one-dimensional models. After an initial transient, thermal equilibrium with the thermostats was established and a stationary heat flux along the chain appeared. A local temperature is numerically defined as $T_n = \langle (\mathbf{R}_n, \dot{\mathbf{R}}_n) \rangle_t / 3$ and the local heat flux as $J_n = \Delta z \langle j_n \rangle_t$, where

$$j_n = -(\dot{\mathbf{R}}_{n+1}, \partial V(\rho_n) / \partial \mathbf{R}_{n+1}) - (\mathbf{F}_{3,n} + \mathbf{F}_{2,n+1}, \dot{\mathbf{R}}_{n+1}) - (\mathbf{F}_{3,n+1}, \dot{\mathbf{R}}_{n+2}) - 3(\dot{\mathbf{R}}_{n+3}, \partial W(r_n) / \partial \mathbf{R}_{n+3}),$$

vector $\mathbf{F}_{2,n} = \partial U(\theta_n) / \partial \mathbf{R}_n$, $\mathbf{F}_{3,n} = \partial U(\theta_n) / \partial \mathbf{R}_{n+1}$. In numerical simulations we used the following values of temperature $T_{\pm} = (1 \pm 0.1)T$, $T = 0.0005$, the relaxation coefficient $\gamma = 0.1$, the number of units $N_{\pm} = 40$, $N = 20, 40, 80, \dots, 2560$.

Dependence of the heat conduction coefficient κ on the length of the free helix segment N was computed according to Eq. (4). The heat conduction coefficient for the helix diverges in the thermodynamic limit. For initial state of the system with $\Delta z = \Delta z_0 = 0.6573$, one observes $\kappa(N) \sim N^{0.20}$, for $N \rightarrow \infty$, and for the stretched helix with $\Delta z = 0.75$, $\kappa(N) \sim N^{0.11}$; for $N \rightarrow \infty$, see Fig. 20. Thus,

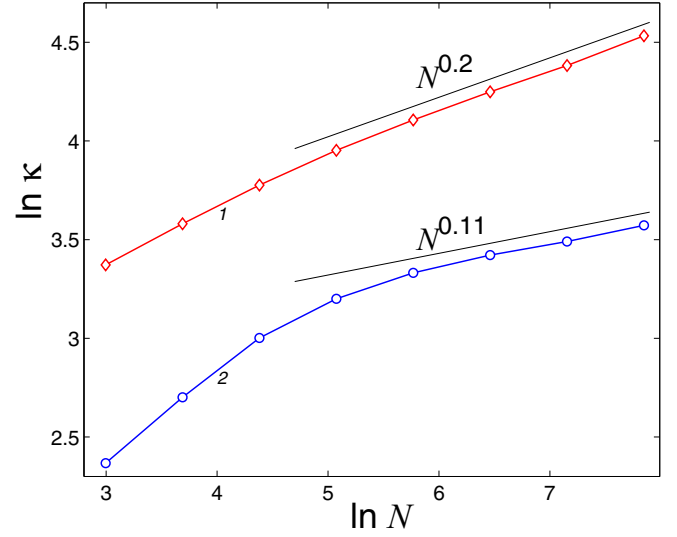


FIG. 20. (Color online) Dependence of the heat-conduction coefficient κ on the size of the internal chain fragment N for α helix with the average longitudinal step $\Delta z = \Delta z_0 = 0.6573$ and $\Delta z = 0.75$ (curves 1 and 2, respectively).

the stretching should bring about a decrease in the heat conductivity.

This result is illustrated in Fig. 21. In this simulation, we choose $N = 320$ and fix a value of the average helix step Δz for each run. As one can see, the stretching of the helix indeed brings about the reduction of the heat flux (and, accordingly, of the heat conduction coefficient). Maximum reduction is achieved approximately for $\Delta z = (\Delta z_1 + \Delta z_2) / 2 = 0.749$, where the lack of homogeneity is the most significant. Further stretching leads to monotonous growth of the heat flux. The strongest reduction of the heat conductivity is achieved for stretching deformation of about $10 \div 13\%$.

As we see, the three-dimensional structure of the model helix does not bring about any qualitatively new phenomena related to the heat conduction. Still, the reduction of the heat conductivity is less profound than it was for the

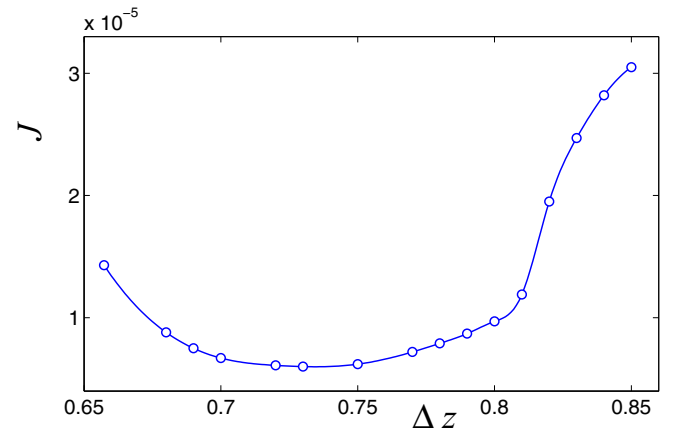


FIG. 21. (Color online) Dependence of the heat flow J on the helix longitudinal step Δz (size of the internal chain fragment $N = 320$, size of edge fragments $N_{\pm} = 40$, edge temperatures $T_{\pm} = 0.0005 \pm 0.00005$).

one-dimensional models considered above. That can be attributed to the fact that the 3D helix has a number of competing “channels” for the heat transfer related to different phonon branches, and the stretching effects only a part of them. As it was already mentioned above, one should expect similar behavior in other systems, which exhibit the nonhomogeneous stretching, such as DNA double-helix and helical proteins [35], as well as in NiAl single-crystal nanofilms [37].

VII. CONCLUDING REMARKS

In this paper we demonstrated that one can efficiently control the transport properties of model atomic chains by application of mechanical load. In the case of the chain with double-well interparticle potential, it is enough to change the average interparticle distance in order to modify a number of possible degenerate ground states and to reduce or to increase the heat conductivity. The effect is rather pronounced (about fivefold reduction was observed). However, even stronger effect—reduction by two orders of magnitude—was observed in more generic model with single-well nonconvex interparticle potential. In this model the heat conductivity is directly related to applied external strain. Also in this case it seems that the reduction effect is caused by formation of “effective” double-well potential and variation of a number of possible states of mechanical equilibrium. The effect was shown to

persist (although to lower extent) for the three-dimensional model of polymer α helix.

Modification of thermal conductivity in conditions of external mechanical load can be related to broader field of thermoelasticity. It is well-known that elasticity and plasticity in real materials can be strongly coupled with thermodynamic phenomena and heat transport. It seems, however, that this possible coupling has not received proper attention in numerous recent studies devoted to microscopic foundations of the heat conductivity. Our results demonstrate that these effects can be rather profound. One can be tempted to say that the extension of the chain with the DW potential exemplifies the effect of plasticity on the heat transport. The chain with the single-well potential requires constant external forcing to reduce the heat conductivity; this phenomenon is primarily elastic. Needless to say, these statements are quite crude and schematic; still we believe that the subject is of considerable fundamental interest. Besides, interesting practical implications are straightforward—one can be interested in simple mechanical means of control over heat transport in micro- and nanosystems.

ACKNOWLEDGMENTS

The authors are grateful to Israel Science Foundation (Grant No. 838/13) for financial support. A.V.S. is grateful to the Joint Supercomputer Center of the Russian Academy of Sciences for the use of computer facilities.

-
- [1] S. Lepri, R. Livi, and A. Politi, *Phys. Rep.* **377**, 1 (2003).
 - [2] N. Li, J. Ren, L. Wang, G. Zhang, P. Hanggi, and B. Li, *Rev. Mod. Phys.* **84**, 1045 (2012).
 - [3] E. Fermi, J. Pasta, and S. Ulam, Studies of nonlinear problems. Los Alamos Report No. LA.1940 (1955).
 - [4] S. Lepri, R. Livi, and A. Politi, *Phys. Rev. Lett.* **78**, 1896 (1997).
 - [5] S. Lepri, R. Livi, and A. Politi, *Physica D* **119**, 140 (1998).
 - [6] S. Lepri, R. Livi, and A. Politi, *Europhys. Lett.* **43**, 271 (1998).
 - [7] R. Rubin and W. Greer, *J. Math. Phys.* **12**, 1686 (1971).
 - [8] A. Casher and J. L. Lebowitz, *J. Math. Phys.* **12**, 1701 (1971).
 - [9] A. Dhar, *Phys. Rev. Lett.* **86**, 5882 (2001).
 - [10] A. Dhar, *Phys. Rev. Lett.* **86**, 3554 (2001).
 - [11] A. V. Savin, G. P. Tsironis, and A. V. Zolotaryuk, *Phys. Rev. Lett.* **88**, 154301 (2002).
 - [12] P. Grassberger, W. Nadler, and L. Yang, *Phys. Rev. Lett.* **89**, 180601 (2002).
 - [13] T. Hatano, *Phys. Rev. E* **59**, R1 (1999).
 - [14] B. Hu, B. Li, and H. Zhao, *Phys. Rev. E* **57**, 2992 (1998).
 - [15] A. V. Savin and O. V. Gendelman, *Phys. Rev. E* **67**, 041205 (2003).
 - [16] G. P. Tsironis, A. R. Bishop, A. V. Savin, and A. V. Zolotaryuk, *Phys. Rev. E* **60**, 6610 (1999).
 - [17] B. Hu, B. Li, and H. Zhao, *Phys. Rev. E* **61**, 3828 (2000).
 - [18] K. Aoki and D. Kuznezov, *Phys. Lett. A* **265**, 250 (2000).
 - [19] O. V. Gendelman and A. V. Savin, *Phys. Rev. Lett.* **92**, 074301 (2004).
 - [20] C. Giardinà, R. Livi, A. Politi, and M. Vassalli, *Phys. Rev. Lett.* **84**, 2144 (2000).
 - [21] O. V. Gendelman and A. V. Savin, *Phys. Rev. Lett.* **84**, 2381 (2000).
 - [22] Y. Zhong, Y. Zhang, J. Wang and H. Zhao, *Phys. Rev. E* **85**, 060102(R) (2012).
 - [23] S. Chen, Y. Zhang, J. Wang, and H. Zhao, [arXiv:1204.5933v3](https://arxiv.org/abs/1204.5933v3).
 - [24] L. Wang, B. Hu, and B. Li, *Phys. Rev. E* **88**, 052112 (2013).
 - [25] S. G. Das, A. Dhar, and O. Narayan, [arXiv:1308.5475](https://arxiv.org/abs/1308.5475).
 - [26] A. V. Savin and Y. A. Kosevich, [arXiv:1307.4725](https://arxiv.org/abs/1307.4725).
 - [27] C. W. Chang, D. Okawa, A. Majumdar, and A. Zettl, *Science* **314**, 1121 (2006).
 - [28] J. Wang, L. Zhu, J. Chen, B. Li, and J. T. L. Thong, *Adv. Mater.* **25**, 6884 (2013).
 - [29] R. Kubo, M. Toda, and N. Hashitsume, *Statistical Physics II*, Vol. 31 (Springer, Berlin, 1991).
 - [30] A. Fillipov, B. Hu, B. Li, and A. Zeltser, *J. Phys. A: Math. Gen.* **31**, 7719 (1998).
 - [31] F. Legoll, M. Luskin, and R. Moeckel, *Nonlinearity* **22**, 1673 (2009).
 - [32] D. Roy, *Phys. Rev. E* **86**, 041102 (2012).

- [33] O. V. Gendelman and A. V. Savin, [Phys. Rev. E **81**, 020103 \(2010\)](#).
- [34] O. V. Gendelman, R. Shvartsman, B. Madar, and A. V. Savin, [Phys. Rev. E **85**, 011105 \(2012\)](#).
- [35] A. V. Savin, I. P. Kikot, M. A. Mazo, and A. V. Onufriev, [Proc. Natl. Acad. Sci. USA **110**, 2816 \(2013\)](#).
- [36] A. V. Savin, M. A. Mazo, I. P. Kikot, and A. V. Onufriev, [arXiv:1110.3165v2](#).
- [37] R. I. Babicheva, K. A. Bukreeva, S. V. Dmitriev, and K. Zhou, [Comput. Mater. Sci. **79**, 52 \(2013\)](#).
- [38] A. Henry and G. Chen, [Phys. Rev. B **79**, 144305 \(2009\)](#).
- [39] J. Liu and R. Yang, [Phys. Rev. B **86**, 104307 \(2012\)](#).
- [40] P. L. Christiansen, A. V. Zolotaryuk, and A. V. Savin, [Phys. Rev. E **56**, 877 \(1997\)](#).
- [41] A. V. Savin and L. I. Manevitch, [Phys. Rev. E **61**, 7065 \(2000\)](#).